Defect levels from SCAN and MBJ meta-GGA exchange-correlation potentials

Tomáš Rauch,[1] Francisco Munoz,[2,3] Miguel A. L. Marques,[4,5] and Silvana Botti[1,5]
[1]*Institut für Festkörpertheorie und -Optik, Friedrich-Schiller-Universität Jena, 07743 Jena, Germany*
[2]*Center for the Development of Nanoscience and Nanotechnology, 9170124 Santiago, Chile*
[3]*Departamento de Física, Facultad de Ciencias, Universidad de Chile, 7800024 Santiago, Chile*
[4]*Institut für Physik, Martin-Luther-Universität Halle-Wittenberg, 06120 Halle/Saale, Germany*
[5]*European Theoretical Spectroscopy Facility*

(Received 7 April 2021; revised 29 July 2021; accepted 30 July 2021; published 11 August 2021)

For more than a decade the HSE06 hybrid exchange-correlation functional developed by Heyd, Scuseria and Ernzerhof has provided a tool for reliable defect level calculations in density functional theory for which post-processing tools are not necessary, in contrast to previous calculations using semilocal density functionals. One of the main reasons for its reliability is the high precision of HSE06 for band gap calculations. Recently, other functionals from the meta-generalized gradient approximation (meta-GGA) class have been used extensively to calculate the electronic properties of solids. In particular, band gaps can be accurately evaluated with the modified Becke-Johnson (MBJ) potential, and relaxed atomic structures close to experimental findings can be obtained with the strongly constrained and appropriately normed (SCAN) exchange-correlation functional. Both approaches are computationally cheaper than HSE06, and we consider here their performance for defect level calculations. We compare results for the $\epsilon(+/0)$ transition levels of seven donors and $\epsilon(0/-)$ transition levels of four acceptors in group IV semiconductors. We conclude that in certain situations where HSE06 cannot be applied because of excessive computational costs, SCAN and MBJ might provide a good alternative.

DOI: 10.1103/PhysRevB.104.064105

I. INTRODUCTION

Precise calculation of the electronic properties of defects in semiconductors is a key to maintain and improve semiconductor technology, which is an almost inseparable part of our modern lives. Electronics, optoelectronics, photovoltaics, and other technological fields depend on the knowledge of the position of defect electronic levels in the band gap of semiconductors and insulators. For decades, density functional theory [1,2] has been the most important approach to first-principles calculations of electronic and structural properties of matter at the atomic scale. Since the exchange-correlation (XC) part of the total energy functional cannot be written in a closed form, it has to be approximated. Hundreds of XC functionals have been proposed for various purposes, but in solid-state physics the basic local-density approximation (LDA) and generalized gradient approximation (GGA) are mostly used as a standard. While these approximations are useful for calculations of different properties of solid systems and molecules, their Kohn-Sham band structures are known to underestimate the band gap of bulk semiconductors and insulators by ∼50% [3]. This "band gap problem" [4] makes it impossible to accurately predict the in-gap defect levels. One common approach to deal with the problem is to apply "postprocessing" corrections after the LDA/GGA calculation [4–9]. These corrections are often of an empirical character, and they do not allow for predictive automatized calculations. Another possibility is to use higher-order approximations of the XC functionals capable of predicting band gaps with higher accuracy, such as the HSE06 hybrid functional developed by Heyd, Scuseria and Ernzerhof [10–12] or the *GW* approximation of the many-body perturbation theory [13]. Out of these different approaches, the use of the HSE06 hybrid functional remains one of the best choices [14,15], combining good accuracy with a feasible numerical cost.

Since the quality of the band gap prediction is one of the keys to accurate calculations of defect levels, recent large-scale investigations [3,16] suggested that not only HSE06 but also other functionals yielding reliable band gaps should be considered. The modified Becke-Johnson [17] (MBJ) exchange potential together with LDA correlation (MBJLDA) is the XC functional with the smallest error when used for Kohn-Sham band gap calculations. It represents, therefore, an interesting alternative to HSE06 for defect calculations, with the advantage of being numerically cheaper. The strongly constrained and appropriately normed (SCAN) [18] XC functional, another functional of a meta-GGA family, has been increasingly used in solid-state physics in view of its accurate evaluation of formation energies. While the Kohn-Sham band gaps predicted by SCAN yield larger errors than MBJLDA or HSE06, we are still interested in its performance for defect level calculations. So far, only a few defect level calculations using MBJ [19–22] and SCAN [23] have been reported in the literature.

In this work we investigate the accuracy of these two meta-GGA XC functionals for calculations of transition energies of various donor and acceptor defects. We consider the

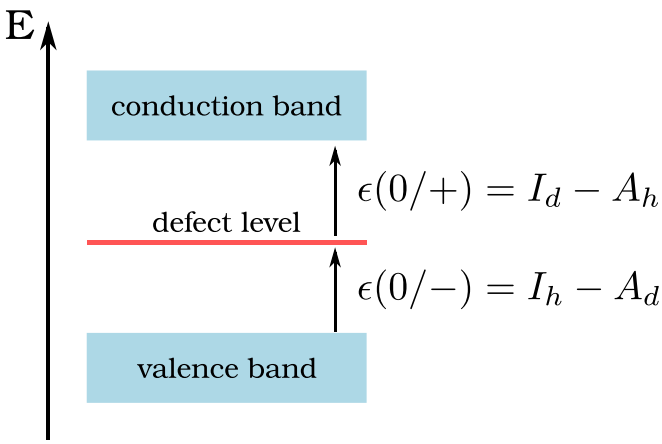

FIG. 1. Sketch of the excitation of a valence electron to an acceptor level and of a donor electron to the conduction band.

substitutional defects in group IV semiconductors previously studied with different methods in Ref. [12] as well as two additional carbon defects investigated in Ref. [24]. We further compare our results with those reported in the above publications (obtained with the HSE06 hybrid functional) and with experimental values.

II. METHODS

To calculate acceptor and donor levels we follow the same approach as Refs. [12,24] to be able to compare our results directly with those obtained in those works with different XC functionals. If we consider the total energy E of a system with N or $N \pm 1$ electrons, we can define the ionization potential I and electron affinity A as

$$I = E(N-1) - E(N), \quad A = E(N) - E(N+1). \tag{1}$$

Using as an approximation the generalized Koopmans theorem [25] valid for the exact XC functional, we further identify the valence band maximum (VBM) ϵ_v and conduction band minimum (CBM) ϵ_c of the perfect host crystal with I and A as

$$\epsilon_c = -A(N) = -I(N+1), \quad \epsilon_v = -I(N). \tag{2}$$

As schematically shown in Fig. 1, we now express the transition level of a neutral donor impurity to a positively charged state (defect-to-conduction-band transition) as

$$\epsilon(0/+) = I_d - A_h = E_d(+) - E_d(0) + \epsilon_c \tag{3}$$

and that of a neutral acceptor impurity to a negatively charged state (valence-band-to-defect transition) as

$$\epsilon(0/-) = I_h - A_d = -\epsilon_v + E_d(-) - E_d(0). \tag{4}$$

The subscripts d and h refer to the defective and host crystals, respectively. This approach is known as the Δ self-consistent field (ΔSCF) method, and it is based on total energy calculations. Equations (3) and (4) can be alternatively derived from the formation energies of the different defect charge states [4].

The MBJLDA functional is only an XC potential; that is, it is not the functional derivative with respect to the density of any XC functional, and as a consequence, it is not possible to calculate total energies with this functional. However, using again the generalized Koopmans theorem [25], one can, in principle, identify I of a defective system with the negative of its highest occupied level (HOMO). In practical calculations where the XC functional has to be approximated, the Koopmans theorem is mostly not fulfilled, leading to the underestimation (LDA/GGA) or overestimation (Hartree-Fock) of the band gaps. The hybrid functionals mix both approximations and benefit from an error cancellation between them [26]. In fact, defect levels can be evaluated with good accuracy with HSE06 even at the Kohn-Sham level [12] (ΔKS approach) as

$$\epsilon(0/+) = -\epsilon_{d,\mathrm{homo}}(0) + \epsilon_c \tag{5}$$

for donors and

$$\epsilon(0/-) = \epsilon_{d,\mathrm{homo}}(-) - \epsilon_v \tag{6}$$

for acceptors. We will determine the precision of the ΔKS approach for the Perdew-Burke-Ernzerhof functional (PBE) [27], MBJLDA, and SCAN and the precision of the ΔSCF approach for PBE and SCAN. All results will be compared with the values obtained in Refs. [12,24] using HSE06 with the ΔSCF approach, as well as with the experimental values cited in those references.

III. COMPUTATIONAL DETAILS

We performed all calculations with the Vienna Ab initio Simulation Package (VASP) code [28] using the projector augmented-wave method [29]. To obtain the bulk properties of the host materials, namely, C, Si, and Ge in the diamond lattice structure, we carried out ground-state calculations on an $11 \times 11 \times 11$ Monkhorst-Pack set of **k** points with the plane-wave cutoff set to 420 eV for C and Ge and 320 eV for Si, including lattice constant relaxation with PBE and SCAN.

To be able to compare our results with Refs. [12,24], defect calculations were performed with the same settings: we used a 512-atom supercell and a Γ-point grid, and the plane-wave cutoff was set to the same values as for the bulk. Again, the atomic positions in the defective supercell were relaxed with PBE and SCAN for both the ground and excited defect states.

For charged supercells, the results have to be corrected to account for the additional contribution to the total energy from the artificial jellium charge, which ensures charge neutrality of the supercell. Following Refs. [12,24], we add to the total energies 65% of the monopole correction [4] $\Delta E_{\mathrm{corr}} = 0.65 \frac{q^2 \alpha_M}{2\epsilon L}$, where q is the charge in the supercell, α_M is the Madelung constant, L is the length of the cubic cell, and ϵ is the dielectric constant, for which we assumed the static experimental value of the host crystal. For cubic supercells this is equivalent to the full correction of Makov and Payne [30], and it has been shown [31] that this correction scheme can be successfully applied to defects with moderate localization. Note that a number of alternative approaches have been proposed in the last decade [32]. Recently, corrections involving ionic contributions were proposed in Refs. [33,34]. While possibly important for multiatomic

TABLE I. Lattice constants a (in Å) and band gaps E_g (in eV) of the host materials calculated with different XC functionals. HSE06 and experimental E_g values are from Ref. [12]; experimental a values are from Ref. [37].

Host	Parameter	PBE	SCAN	MBJ_{PBE}	MBJ_{SCAN}	HSE06	Expt
C	a	3.56	3.55				3.57
	E_g	4.17	4.60	5.00	5.01	5.42	5.48
Si	a	5.47	5.43				5.43
	E_g	0.62	0.84	1.30	1.26	1.17	1.17
Ge	a	5.78	5.68				5.66
	E_g	0.00	0.06	0.33	0.83	0.84	0.74

systems, they can be neglected for defects in elementary bulk crystals. In this paper we concentrate on the role of the meta-GGA functionals, and we leave investigations related to the effect of different charge corrections for further projects.

When the ΔKS method is used for acceptors, the position of the occupied charged defect level has to be modified as well. Assuming that the charge is strongly localized at only the defect, we apply the correction [35] $\Delta\epsilon_{\rm corr} = \frac{2}{q}\Delta E_{\rm corr}$.

Since differences in energies calculated for different systems are used for the charge transition levels, a common reference level has to be defined. To this end we align the electrostatic potentials averaged over the unit cells of the individual systems [36].

Finally, since the $\epsilon(0/+)$ donor level is calculated from ground-state properties only in the ΔKS approach [see Eq. (5)], we add the relaxation energy of the charged defect to obtain the adiabatic charge transition levels that can be compared with the experimental values. The relaxation energy is evaluated as the difference in total energies of the charged defect before and after structural relaxation. Total energies obtained with PBE or SCAN are applied also to MBJLDA calculations because they cannot be calculated directly with the latter.

TABLE II. Calculated position of the donor and acceptor defect levels $\epsilon(+/0)$ and $\epsilon(0/-)$ with respect to CBM and VBM, respectively. The absolute error (AE) is calculated with respect to experimental values from Refs. [12,24] and references therein. The numbers in parentheses are absolute relative errors in percent. The asterisk (*) indicates that the calculated defect level does not lie in the band gap of the host material as calculated by the given XC functional (see text for further details). Ge:S is excluded for the calculation of the mean errors in the case of PBE and SCAN.

Donors

		PBE		SCAN		MBJ_{PBE}		MBJ_{SCAN}		HSE06		Expt
	Method	$\epsilon(+/0)$	AE (%)	$\epsilon(+/0)$	AE (%)	$\epsilon(+/0)$	AE (%)	$\epsilon(+/0)$	AE (%)	$\epsilon(+/0)$	AE (%)	$\epsilon(+/0)$
C:N	ΔSCF	−1.31	0.39 (23)	−1.65	0.05 (3)					−1.8	0.1 (6)	−1.7
	ΔKS	−0.59	1.11 (65)	−0.98	0.72 (42)	−1.21	0.49 (29)	−1.19	0.51 (30)			
C:V	ΔSCF	−3.55	0.75 (18)	−4.14	0.16 (4)					−4.4	0.1 (2)	−4.3
	ΔKS	−3.19	1.11 (26)	−3.74	0.56 (13)	−4.29	0.01 (0)	−4.27	0.03 (0)			
C:P	ΔSCF	−0.42	0.16 (27)	−0.43	0.15 (27)					−0.52	0.06 (10)	−0.58
	ΔKS	−0.18	0.40 (69)	−0.18	0.40 (69)	−0.12	0.46 (79)	−0.12	0.46 (80)			
Si:Au	ΔSCF	−0.38	0.43 (53)	−0.56	0.25 (30)					−0.75	0.06 (7)	−0.81
	ΔKS	−0.28	0.53 (65)	−0.44	0.37 (45)	−0.75	0.06 (7)	−0.70	0.11 (13)			
Ge:S	ΔSCF	−0.07*	0.21 (76)	−0.04	0.24 (84)					−0.29	0.01 (4)	−0.28
	ΔKS	*		*		−0.06	0.22 (78)	−0.29	0.01 (3)			
Si:S	ΔSCF	−0.24	0.08 (24)	−0.26	0.06 (18)					−0.26	0.06 (19)	−0.32
	ΔKS	−0.21	0.11 (35)	−0.22	0.10 (30)	−0.27	0.05 (17)	−0.39	0.07 (23)			
Si:S+	ΔSCF	−0.39	0.20 (34)	−0.45	0.14 (24)					−0.54	0.05 (8)	−0.59
	ΔKS	−0.39	0.20 (33)	−0.45	0.14 (24)	−0.51	0.08 (14)	−0.51	0.08 (13)			
Mean	ΔSCF		0.34 (30)		0.14 (18)						0.06 (8)	
	ΔKS		0.58 (47)		0.38 (37)		0.20 (32)		0.18 (23)			

Acceptors

		PBE		SCAN		MBJ_{PBE}		MBJ_{SCAN}		HSE06		Expt
	Method	$\epsilon(0/-)$	AE (%)	$\epsilon(0/-)$	AE (%)	$\epsilon(0/-)$	AE (%)	$\epsilon(0/-)$	AE (%)	$\epsilon(0/-)$	AE (%)	$\epsilon(0/-)$
C:B	ΔSCF	0.29	0.08 (22)	0.29	0.08 (23)					0.36	0.01 (3)	0.37
	ΔKS	0.41	0.04 (11)	0.41	0.04 (10)	0.41	0.04 (11)	0.41	0.04 (12)			
Si:O	ΔSCF	0.63*	0.32 (33)	0.85*	0.10 (11)					0.88	0.07 (7)	0.95
	ΔKS	*		*		*		*				
Si:In	ΔSCF	0.16	0.01 (5)	0.17	0.02 (14)					0.15	0.0 (0)	0.15
	ΔKS	0.16	0.01 (9)	0.18	0.03 (19)	0.22	0.07 (43)	0.25	0.10 (65)			
Ge:O	ΔSCF	0.0*	0.32 (99)	0.18*	0.14 (44)					0.34	0.02 (6)	0.32
	ΔKS	*		*		*		*				

IV. RESULTS

We start comparing the results that we obtained for the host crystals C, Si, and Ge, summarized in Table I. First, we see that the experimental lattice constant is reproduced much better with SCAN calculations than with PBE. Second, looking at the bulk band gaps, we confirm that the experimental values are strongly underestimated by PBE and SCAN. Most importantly, a metallic behavior is predicted for Ge by PBE, and only a tiny band gap is open using SCAN. Using MBJLDA, we obtained values much closer to the experimental ones. Note that using the overestimated PBE lattice constant with MBJLDA (MBJ_{PBE}) yields a strongly underestimated Ge band gap. Only with the very precise SCAN lattice constant did we obtain the Ge band gap with satisfying precision using MBJLDA (MBJ_{SCAN}). In all three cases, HSE06 also gives band gap values close to the experimental ones [12]. These

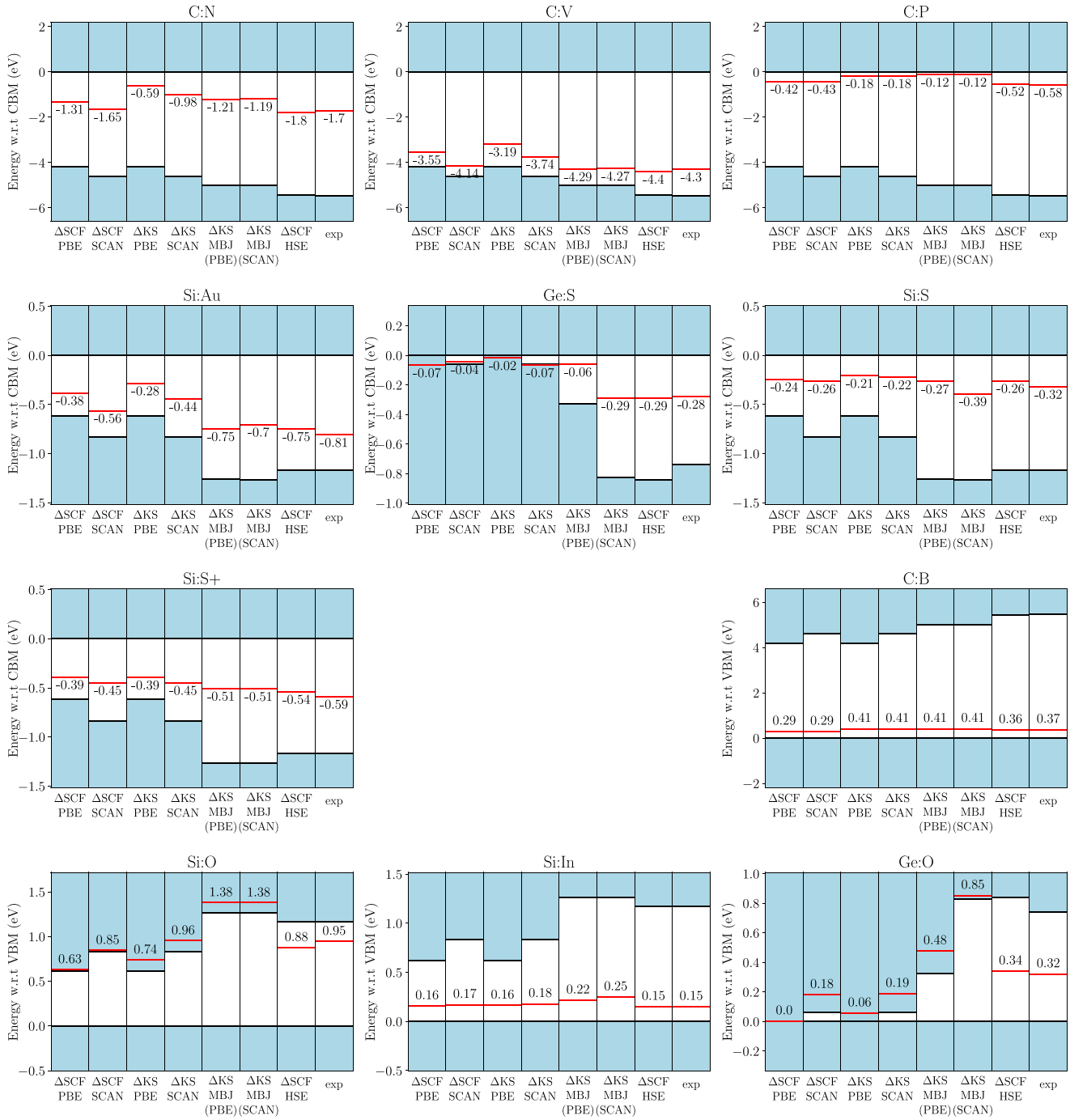

FIG. 2. The position of the adiabatic $\epsilon(+/0)$ and $\epsilon(0/-)$ charge transition levels (red) with respect to the host band edges for seven donors and four acceptors calculated with different XC functionals and from experimental measurement. In blue are presented the host valence and conduction bands.

findings are in agreement with the general performance of these XC functionals [3,16,38].

Let us now turn to the results we obtained for the defect energy levels that we summarize in Table II.

We considered seven different donor substitution defects (C:N, C:V, C:P, Si:S, Si:S+, Si:Au, Ge:S) and four different acceptor substitution defects (C:B, Si:O, Si:In, Ge:O) which were previously utilized to evaluate the quality of HSE06 for defect level calculations in Ref. [12] as well as to better understand the carbon nitrogen-vacancy defect in Ref. [24]. The authors of Ref. [12] concluded that HSE06 yields very precise results, mostly within 0.1 eV with respect to the experimental values for both ΔSCF and ΔKS approaches. We will compare the PBE, SCAN, MBJ_{PBE}, and MBJ_{SCAN} results with the HSE06 and experimental values obtained for adiabatic transitions. Thus, relaxation of the excited states is included.

We first discuss the calculations for donors. All results are presented graphically in Fig. 2. Note that in the ΔKS approach charge corrections are not necessary in this case with the exception of the Si:S+ defect. For defects in C and Si hosts the ΔSCF PBE and SCAN results differ from experimental values by 0.34 eV (23%) and 0.14 eV (18%), respectively, whereas with the ΔKS approach we obtained differences of 0.58 eV (47%) and 0.38 eV (37%) for PBE and SCAN, respectively. This demonstrates that these XC functionals do not fulfill the generalized Koopmans theorem. The ΔKS values obtained with MBJ_{PBE} [0.20 eV (32%)] and MBJ_{SCAN} [0.18 eV (23%)] are better than those of PBE and SCAN in the ΔKS approach and even those of PBE in the ΔSCF approach, but they are worse than the SCAN ΔSCF results. For the Ge:S defect, PBE and SCAN do not predict any defect levels in the band gap, and MBJ_{PBE} underestimates its position with respect to the CBM due to the severe underestimation of the Ge band gap. In this situation, a reasonable result can be obtained only with MBJ_{SCAN}. We observe that the SCAN ΔSCF approach is the best, on average, in situations where the band gap is not underestimated too strongly. If it is the case, such as for Ge:S and Si:Au, MBJLDA can yield results close to the experimental value due to its good prediction of the host band gap (i.e., in combination with SCAN for ionic relaxation or directly for experimental ionic positions). In all cases, HSE06 remains superior to the XC functionals considered in this work.

We now turn to the acceptors. All results are presented graphically in Fig. 2. In this case, both the ΔSCF and ΔKS approaches include charge corrections. First, we note that for Si:O and Ge:O, all considered functionals predict the defect level outside of the host band gap, even though MBJ_{SCAN} yields almost the experimental band gap value in both cases. Possibly, this behavior is related to some specific properties of the oxygen defect. For the other defects, the picture we obtained is much less clear than in the case of the donors. For C:B, PBE and SCAN in the ΔSCF approach yield $\epsilon(0/-)$, which underestimates the experimental value by 0.08 eV, and in the ΔKS approach the value is overestimated by 0.04 eV identically by all four functionals, resulting in a satisfactory result. For Si:In, PBE and SCAN yield results fairly close to the experiment in both the ΔSCF and ΔKS approaches, and it is slightly overestimated by MBJ_{PBE} and MBJ_{SCAN} in the ΔKS approach. Including the results for Si:O and Ge:O in the discussion, we can carefully draw the conclusion that PBE and SCAN tend to underestimate $\epsilon(0/-)$, whereas it is rather overestimated by MBJLDA. As for the donors, HSE06 with absolute errors below 0.1 eV is better than the PBE, SCAN, or MBJ XC functionals.

V. CONCLUSION

We performed defect level calculations for several donor and acceptor impurities in group IV semiconductors and investigated the reliability of the PBE, SCAN, and MBJLDA XC functionals using either PBE or SCAN geometries in comparison to HSE06 calculations and experimental results. We found that for donors SCAN is the best option in the ΔSCF approach when the host band gap is not underestimated too strongly. For deep defect levels MBJ_{SCAN} becomes the best option, as a result of the very good precision of MBJLDA for band gap prediction. For acceptor energy levels PBE and SCAN tend to underestimate the defect level position with respect to the valence band maximum, whereas this value is rather overestimated by MBJLDA. Note that these results provide only a first hint of the accuracy of the tested functionals, and more defect systems should be studied to obtain a more general picture. In addition to MBJLDA, we also performed calculations with the local MBJ (LMBJ) XC functional introduced recently [39]. The results obtained with MBJ and LMBJ are very similar. The reason is the local mixing parameter of LMBJ cannot be averaged over a region smaller than a typical bulk unit cell, and it thus remains almost constant in the defective system, as in the case of the global MBJLDA functional.

We conclude that neither of the tested meta-GGA XC functionals performs as good as HSE06 for defect level calculations: hybrid functionals should therefore remain one of the primary choices if computationally feasible for the class of systems that we have considered. For very large supercells HSE06 may become numerically too expensive. In such situations we identify the SCAN XC functional in the ΔSCF approach as a reasonable compromise, if the host band gap is well reproduced and the defect level is shallow. On the other hand, if the considered defect level lies rather deep in the host band gap, we identified the MBJLDA XC potential as a possible alternative to HSE06. In this case, atomic relaxations should be performed using SCAN or another functional that gives accurate lattice constants.

ACKNOWLEDGMENTS

This work was supported by the Deutsche Forschungsgemeinschaft (DFG, German Research Foundation) through Projects No. SFB-1375 (Project No. A02) and No. BO 4280/8-1. S.B. and T.R. also acknowledge funding from the Volkswagen Stiftung (Momentum) through the project "dandelion." F.M. was supported by Fondecyt Grant No. 1191353, by the Center for the Development of Nanoscience and Nanotechnology Grant No. AFB180001, by Conicyt PIA/Anillo Grant No. ACT192023, and by the supercomputing infrastructure of the NLHPC (ECM-02).

[1] P. Hohenberg and W. Kohn, Phys. Rev. **136**, B864 (1964).
[2] W. Kohn and L. J. Sham, Phys. Rev. **140**, A1133 (1965).
[3] P. Borlido, T. Aull, A. W. Huran, F. Tran, M. A. L. Marques, and S. Botti, J. Chem. Theory Comput. **15**, 5069 (2019).
[4] S. Lany and A. Zunger, Phys. Rev. B **78**, 235104 (2008).
[5] A. Janotti and C. G. Van de Walle, Phys. Rev. B **76**, 165202 (2007).
[6] S. Lany, H. Raebiger, and A. Zunger, Phys. Rev. B **77**, 241201(R) (2008).
[7] S. Lany and A. Zunger, Phys. Rev. B **72**, 035215 (2005).
[8] T. R. Paudel and W. R. L. Lambrecht, Phys. Rev. B **77**, 205202 (2008).
[9] C. D. Pemmaraju, R. Hanafin, T. Archer, H. B. Braun, and S. Sanvito, Phys. Rev. B **78**, 054428 (2008).
[10] J. Heyd, G. E. Scuseria, and M. Ernzerhof, J. Chem. Phys. **118**, 8207 (2003).
[11] J. Heyd, G. E. Scuseria, and M. Ernzerhof, J. Chem. Phys. **124**, 219906 (2006).
[12] P. Deák, B. Aradi, T. Frauenheim, E. Janzén, and A. Gali, Phys. Rev. B **81**, 153203 (2010).
[13] S. Lany and A. Zunger, Phys. Rev. B **81**, 113201 (2010).
[14] J. L. Lyons and C. G. Van de Walle, npj Comput. Mater. **3**, 12 (2017).
[15] P. Deák, M. Lorke, B. Aradi, and T. Frauenheim, J. Appl. Phys. **126**, 130901 (2019).
[16] P. Borlido, J. Schmidt, A. W. Huran, F. Tran, M. A. L. Marques, and S. Botti, npj Comput. Mater. **6**, 96 (2020).
[17] F. Tran and P. Blaha, Phys. Rev. Lett. **102**, 226401 (2009).
[18] J. Sun, A. Ruzsinszky, and J. P. Perdew, Phys. Rev. Lett. **115**, 036402 (2015).
[19] M. Boujnah, H. Ennaceri, A. El Kenz, A. Benyoussef, E. Chavira, M. Loulidi, and H. Ez-Zahraouy, J. Comput. Electron. **19**, 940 (2020).
[20] C. E. Ekuma, J. Phys. Chem. Lett. **9**, 3680 (2018).
[21] J. Hoya, J. Laborde, D. Richard, and M. Rentería, Comput. Mater. Sci. **139**, 1 (2017).
[22] F. Karsai, P. Tiwald, R. Laskowski, F. Tran, D. Koller, S. Gräfe, J. Burgdörfer, L. Wirtz, and P. Blaha, Phys. Rev. B **89**, 125429 (2014).
[23] Y. Zhang, J. W. Furness, B. Xiao, and J. Sun, J. Chem. Phys. **150**, 014105 (2019).
[24] P. Deák, B. Aradi, M. Kaviani, T. Frauenheim, and A. Gali, Phys. Rev. B **89**, 075203 (2014).
[25] C.-O. Almbladh and U. von Barth, Phys. Rev. B **31**, 3231 (1985).
[26] S. Lany and A. Zunger, Phys. Rev. B **80**, 085202 (2009).
[27] J. P. Perdew, K. Burke, and M. Ernzerhof, Phys. Rev. Lett. **77**, 3865 (1996).
[28] G. Kresse and J. Furthmüller, Phys. Rev. B **54**, 11169 (1996).
[29] G. Kresse and D. Joubert, Phys. Rev. B **59**, 1758 (1999).
[30] G. Makov and M. C. Payne, Phys. Rev. B **51**, 4014 (1995).
[31] H.-P. Komsa, T. T. Rantala, and A. Pasquarello, Phys. Rev. B **86**, 045112 (2012).
[32] A. Walsh, npj Comput. Mater. **7**, 72 (2021).
[33] T. Gake, Y. Kumagai, C. Freysoldt, and F. Oba, Phys. Rev. B **101**, 020102(R) (2020).
[34] S. Falletta, J. Wiktor, and A. Pasquarello, Phys. Rev. B **102**, 041115(R) (2020).
[35] W. Chen and A. Pasquarello, Phys. Rev. B **88**, 115104 (2013).
[36] S. E. Taylor and F. Bruneval, Phys. Rev. B **84**, 075155 (2011).
[37] T. Hom, W. Kiszenik, and B. Post, J. Appl. Crystallogr. **8**, 457 (1975).
[38] G. Zhang, A. M. Reilly, A. Tkachenko, and M. Scheffler, New J. Phys. **20**, 063020 (2018).
[39] T. Rauch, M. A. L. Marques, and S. Botti, J. Chem. Theory Comput. **16**, 2654 (2020).